



Gene expression profiling and in vitro functional studies reveal *RAD54L* as a potential therapeutic target in multiple myeloma

Ivyna Pau Ni Bong¹ · Ching Ching Ng² · Norodiyah Othman¹ · Ezalia Esa¹

Received: 22 October 2021 / Accepted: 11 May 2022 / Published online: 11 June 2022
© The Author(s) 2022

Abstract

Background Current advances in the molecular biology of multiple myeloma (MM) are not sufficient to fully delineate the genesis and development of this disease.

Objective This study aimed to identify molecular targets underlying MM pathogenesis.

Methods mRNA expression profiling for 29 samples (19 MM samples, 7 MM cell lines and 3 controls) were obtained using microarray. We evaluated the in vitro effects of *RAD54L* gene silencing on the proliferation, apoptosis and cell cycle distribution in KMS-28BM human MM cells using siRNA approach. Cell proliferation was determined by MTS assay while apoptosis and cell cycle distribution were analysed with flow cytometry. Gene and protein expression was evaluated using RT-qPCR and ELISA, respectively.

Results Microarray results revealed a total of 5124 differentially expressed genes (DEGs), in which 2696 and 2428 genes were up-regulated and down-regulated in MM compared to the normal controls, respectively (fold change ≥ 2.0 ; $P < 0.05$). Up-regulated genes (*RAD54L*, *DIAPH3*, *SHCBP1*, *SKA3* and *ANLN*) and down-regulated genes (*HKDC1*, *RASGRF2*, *CYSLTR2*) have never been reported in association with MM. Up-regulation of *RAD54L* was further verified by RT-qPCR ($P < 0.001$). In vitro functional studies revealed that *RAD54L* gene silencing significantly induced growth inhibition, apoptosis (small changes) and cell cycle arrest in G0/G1 phase in KMS-28BM ($P < 0.05$). Silencing of *RAD54L* also decreased its protein level ($P < 0.05$).

Conclusions This study has identified possible molecular targets underlying the pathogenesis of MM. For the first time, we reveal *RAD54L* as a potential therapeutic target in MM, possibly functioning in the cell cycle and checkpoint control.

Keywords Multiple myeloma · Differentially expressed genes · *RAD54L* · Cell proliferation · Apoptosis · Cell cycle

Introduction

Multiple myeloma (MM) is a cancer of plasma cells. It is a highly heterogeneous and genetically complex form of blood cancer (Corre et al. 2015). MM is the second leading cause of haematological malignancy in the world (de Mel et al. 2014). Development and progression of MM required multiple primary and secondary oncogenic events. Hyperdiploidy and translocations concerning the IgH locus are

frequent primary genetic events in the initiation of MM disease. IgH translocations frequently lead to the activation of proto-oncogenes for instance *FGFR3/MMSET*/t(4;14), *CCND1*/t(11;14), *c-MAF/CCND2*/t(14;16), *MAF-B*/t(14;20) and *CCND3*/t(6;14) (Colombo et al. 2015; Pinto et al. 2020). Acquired mutations (*K-RAS*, *N-RAS*, *BRAF*, *DIS3*, *FAM46C* and *TP53* genes), copy number aberrations (del(17p)/TP53, del(13) and 1q gain), NF- κ B pathway mutation and *MYC* aberrations are recurrent secondary oncogenic events in MM, which are associated with disease progression (Colombo et al. 2015; Roy et al. 2018; Pinto et al. 2020).

Current advances in research have dramatically expanded our understanding of the genomic landscape, tumour heterogeneity and clonal evolution in MM (Furukawa and Kikuchi 2020). However, MM remains incurable with a poor prognosis due to a lack of suitable tumour markers for early diagnosis and treatment. Therefore, identifying new

✉ Ivyna Pau Ni Bong
ivyna@moh.gov.my

¹ Haematology Unit, Cancer Research Centre, Institute for Medical Research, National Institutes of Health, Ministry of Health Malaysia, 40170 Shah Alam, Selangor, Malaysia

² Faculty of Science, Institute of Biological Sciences, University of Malaya, Kuala Lumpur, Malaysia

tumour biomarkers and therapeutic targets are essential steps to improve the prognostic and outcomes of patients. The aims of this study are to identify molecular targets underlying the pathogenesis of MM by mRNA expression profiling and functional target validation by using siRNA and cell-based assays.

Materials and methods

Patient samples

Bone marrow or whole blood were taken from MM patients (N = 19: MM1–MM19) and healthy donors (N = 3: NB1, NB2, and NB3) and stored at -80°C . The average age of the patient was 57 years while the median age was 61 years. The age of the patients was in the range of 28–74 years. Seventeen patients were newly diagnosed MM (NDMM), 2 were from relapsed MM cases. Patients were with > 10% plasma cell infiltration at the time of sample recruitment. Cytogenetic analysis indicated 13 patients with normal karyotype, 1 patient with hypodiploidy and 5 patients with unknown karyotype. Patients' clinical parameters are shown in Table 1.

Cell lines

The U-266, RPMI-8226, IM-9 and MM.1S cells were obtained from American Type Culture Collection (ATCC, USA). The KMS-28BM, KMS-12BM and KMS-20 were purchased from the Japanese Collection of Research Bioresources (JCRB) cell bank. Multiple myeloma cells were cultured and maintained in RPMI-1640 medium (PAN-Biotech, Germany) with 10% fetal bovine serum (Sigma-Aldrich, Germany) in an incubator at 37°C with 5% CO_2 . Cells were sub-cultured when achieved 70–75% confluence. Cells at the logarithmic phase were used for transfection.

Isolation of total RNAs

Total RNAs were isolated from the bone marrow/peripheral blood/cells according to manufacturer's recommendation (Qiagen RNeasy mini kit). DNA digestion was performed to ensure that the RNA was free of DNA contamination (Qiagen DNase I, Hilden, Germany). The integrity of the total RNAs used for gene expression microarray were checked with Bioanalyser (RNA Nano Chip, Agilent 2100 Bioanalyser). All samples included in the gene expression microarray had an RNA integrity number (RIN) of at least 8.0. The purity of the isolated Total RNAs was also checked with NanoDrop ND-1000 UV–VIS spectrophotometer to ensure that the purity was within the range of 1.80–2.10.

Table 1 Clinical parameters for 19 multiple myeloma patients

Patient ID	Age at diagnosis	Race	Gender	Cytogenetic analysis	NDMM/ relapsed MM
MM1	68	Malay	F	No chromosomal abnormality observed	NDMM
MM2	30	Others	M	No chromosomal abnormality observed	NDMM
MM3	64	Malay	F	No chromosomal abnormality observed	NDMM
MM4	74	Chinese	M	No chromosomal abnormality observed	NDMM
MM5	59	Malay	M	No chromosomal abnormality observed	NDMM
MM6	48	Others	M	No chromosomal abnormality observed	NDMM
MM7	28	Malay	M	No chromosomal abnormality observed	NDMM
MM8	48	Malay	F	Unknown	NDMM
MM9	62	Malay	F	Unknown	NDMM
MM10	64	Malay	F	No chromosomal abnormality observed	Relapsed MM
MM11	61	Chinese	M	Unknown	Relapsed MM
MM12	70	Malay	F	No chromosomal abnormality observed	NDMM
MM13	72	Others	M	No chromosomal abnormality observed	NDMM
MM14	51	Others	F	No chromosomal abnormality observed	NDMM
MM15	65	Malay	F	Hypodiploidy with multiple abnormalities	NDMM
MM16	61	Chinese	M	No chromosomal abnormality observed	NDMM
MM17	51	Others	M	Unknown	NDMM
MM18	48	Malay	M	Unknown	NDMM
MM19	62	Malay	F	No chromosomal abnormality observed	NDMM

MM multiple myeloma, NDMM newly diagnosed multiple myeloma

Gene expression microarray assay

Sample processing, labelling, and hybridisation were performed following the standard protocol recommended by Agilent's manufacturer. Approximately 60,000 probes were contained on each array. Briefly, 100 ng of total RNAs were labelled using one colour Agilent's Low Input Quick Amp Labelling kit and purified with spin column (Qiagen RNeasy mini kit, Hilden, Germany). Hybridisation was performed using 600 ng of labelled cRNAs onto SurePrint G3 Human GE 8 × 60 K V2 Microarray Kit (Agilent Technologies, USA). The microarray slide was then put into an incubator with rotation at 65 °C for 17 h. Microarray images were scanned and data from raw microarray image files were extracted with Agilent Feature Extraction Software Version 10.7.3.1 to prepare for analysis. Only samples that passed the raw data quality control metrics as described by Agilent's recommended procedure were proceeded to data analysis. Pre-processing of the data files in this study was performed by using GeneSpring software version 14.9. All the raw data were thresholded to 1 and normalised to the 75th percentile. This was followed by a baseline transformation set to the median of all samples.

Significantly differentially expressed probes in MM vs. normal controls were identified by unpaired unequal variance *t*-test (Welch) ($P < 0.05$). The Benjamini Hochberg false discovery rate (FDR) multiple testing corrections was used to identify differentially expressed probes. The resulting list was further refined by analysing it to a second filter, which specified a 2.0-fold change between MM vs. controls. Only probes that passed a *p*-value cut-off of 0.05 and fold change ≥ 2.0 were considered significant. Unsupervised hierarchical clustering analysis was carried out for the up-regulated and down-regulated probes, respectively, with a *p*-value cut-off of 0.05 and fold change ≥ 2.0 . Unsupervised hierarchical clustering was generated using Euclidean distance metric and average linkage statistical methods.

In vitro functional study of *RAD54L* in KMS-28BM human MM cell line

siRNA transfection

Three target-specific siRNA oligo duplexes (Cohesion Biosciences, Catalog No.: CRH5528) of the human *RAD54L* gene were pooled together to knockdown the target gene in KMS-28BM MM cells. Briefly, 2×10^6 cells were resuspended in 100 μ l of 4D-Nucleofector™ solution (Lonza, USA) and mixed with 500 nM of *RAD54L* siRNA or negative control siRNA. The mixture was transferred to a cuvette. Transfection was then carried out using program DY-100 in a 4D-Nucleofector™ system (Lonza, USA). Then, cells

in the cuvette were gently transferred to warm medium in 24 well plates. Two or three independent experiments were carried out for each transfection.

RT-qPCR analysis

Total RNAs were converted to first strand cDNA following manufacturer's protocol (High Capacity RNA-to-cDNA kit, Applied Biosystems, USA). The RT-qPCR was performed using the TaqMan gene expression assay (Applied Biosystems, USA) in the StepOnePlus™ Real-time PCR System (Applied Biosystems, USA). Pre-designed TaqMan gene expression assays for *RAD54L* (Hs00936473_m1, ThermoFisher Scientific, USA) and internal control *GAPDH* (Hs02758991-g1, ThermoFisher Scientific, USA) were used. Thermal cycling conditions consisted of the following: initial denaturation at 95 °C for 20 s, followed by 40 cycles of 95 °C for 1 s and 60 °C for 20 s. The relative expression of genes was calculated and quantified based on $2^{-\Delta\Delta C_t}$ method.

MTS assay

RAD54L siRNA or negative control siRNA was transfected into KMS-28BM. Cells were seeded onto 96-well plates at a density of 2.0×10^4 cells/well in 100 μ l of culture medium. Cells were cultured for 24 h, 48 h and 72 h. At 0 h and after 24 h, 48 h and 72 h post-transfection, 20 μ l of CellTiter 96 Aqueous One Solution Reagent (Promega, USA) was added into each sample well. The plate was then incubated at 37 °C for 3–4 h in a humidified 5% CO₂ incubator. Subsequently, the plate was measured at absorbances of 490 nm and 630 nm using Synergy HTX microplate reader (BioTek®, USA). The 630 nm reading was then subtracted from the 490 nm reading.

Apoptosis assay

After 48 h of transfection, *RAD54L* siRNA and control siRNA-treated cells were harvested by centrifugation at 1000 rpm. Cells were washed with ice-cold PBS and then resuspended in Annexin binding buffer at 5.0×10^5 cells/mL. This was followed by staining the cells with 5 μ l of Annexin-V-FITC and 5 μ l of propidium iodide (PI) (Elabscience, USA). Finally, the cells were analysed with the FACS-CANTO II flow cytometer (BD BioScience, USA) in which 10,000 events were recorded for each analysis.

Cell-cycle analysis

Briefly, transfection was performed according to the procedure described above. Cells transfected with *RAD54L* siRNA or control siRNA were then transferred to a 24-well cell culture plate containing pre-warm medium. The plate was then

incubated at 37 °C CO₂ cell incubator for 48 h. After 48 h of transfection, cells were harvested and washed with ice-cold PBS. This was followed by fixing the cells with 70% ethanol overnight. Approximately 1×10^5 cells were stained with 500 μ l of PI solution (BD BioScience, USA). The mixture was incubated for 15 min at room temperature. Cell cycle distribution was then analysed with FACSCANTO II flow cytometer (BD BioScience, USA) and ModFit LT (Verity Software House).

The determination of RAD54L protein level with ELISA

Standards were diluted and prepared according to manufacturer's protocol (SUNLONG Human RAD54L ELISA kit). Forty microliters of sample dilution buffer and 10 μ l of sample were added into sample wells and then incubated for 30 min at 37 °C. Then, the wash buffer stock solution was diluted 1:30 in distilled water. Microtiter plate was washed for 30 s, repeatedly for 5 times. This was followed by adding 50 μ l of HRP-conjugate reagent to each sample well. The mixture was then incubated and washed as described above. Then, 50 μ l of each Chromogen Solution A and B were added into the sample well. Subsequently, the plate was incubated for 15 min at 37 °C. This was followed by adding 50 μ l of stop solution to terminate the reaction. Lastly, absorbance was measured at 450 nm with a microplate reader (Tecan Infinite® M1000).

Statistical analysis

Student's *t*-test was used to assess statistical significance between the means of the 2 groups. Those having *P*-value lower than 0.05 were considered significant.

Results

mRNA expression profiling and RT-qPCR verification

mRNA expression profiling was performed for 19 MM samples, 7 MM cell lines and 3 normal controls. A total of 50739 probes were retained after normalising and filtering at selected thresholds. Out of 50739 probes, 5888 probes were significantly differentially expressed ($P < 0.05$; fold change ≥ 2.0). The results are depicted in a volcano plot (Fig. 1A). These 5888 probes were consisted of 5124 genes (including long intergenic non-protein coding RNAs, lincRNAs and novel transcripts). Among 5124 genes, 2696 and 2428 genes were up-regulated and down-regulated in MM vs. the control group, respectively. Genes showing up-regulation and down-regulation in MM vs. controls are listed in Online Resource 1 and Online Resource 2, respectively.

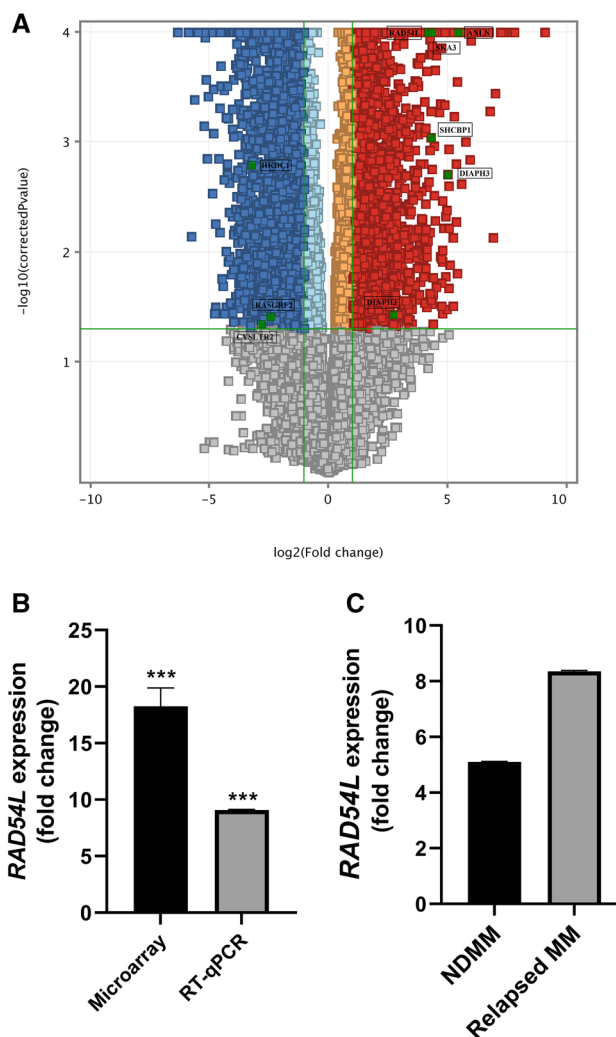


Fig. 1 A Volcano plot identified 5888 differentially expressed probes in multiple myeloma vs. normal controls (fold change ≥ 2.0 ; $P < 0.05$). The *x*-axis represents the \log_2 -fold change of probes, while the *y*-axis represents the $-\log_{10}$ of the corrected *P* values for each probe. Each dot represents a probe and the red- and blue-coloured areas represent the up-regulated and down-regulated probes, respectively, that met the selection criteria of a fold change of at least 2 (fold change ≥ 2.0 or ≤ -2.0) and a $P < 0.05$. Orange and light blue dots represent up-regulated and down-regulated probes that failed to pass the fold change cut-off, respectively. Green dots represent probes for *RAD54L*, *DIAPH3*, *SHCBP1*, *SKA3*, *ANLN*, *HKDC1*, *RASGRF2* and *CYSLTR2*. B Graph showing the mean expression of *RAD54L* detected in microarray and RT-qPCR. *RAD54L* is up-regulated in 23 MM samples as measured by RT-qPCR, consistent with microarray findings. C Graph showing mean expression of *RAD54L* in relapsed MM ($N = 14$) is higher than NDMM ($N = 2$) as determined by RT-qPCR. *** $P < 0.001$

Unsupervised hierarchical clustering was performed on up-regulated and down-regulated genes for all samples, respectively. Genes which expressed at similar patterns were clustered together and joined by a sequence of branches or dendrogram. The genes input list contained DEGs with

a corrected $P < 0.05$ and a fold change of ≥ 2.0 . Online Resources 3 & 4 showing the heatmaps of three distinct sub-clusters classified according to the degree of similarity in gene expression: MM cell lines, MM clinical samples (except MM9 for Online Resource 3; MM5 and MM9 for Online Resource 4) and controls.

The up-regulation of *RAD54L* as detected with microarray analysis was further verified by using RT-qPCR in 23 MM samples from the same cohort (except MM2, MM5 and MM9, where the RNA concentration was insufficient for RT-qPCR). The RT-qPCR results showed that *RAD54L* was significantly up-regulated in the MM vs. control group, consistent with microarray findings ($P < 0.001$) (Fig. 1B). Additionally, when we compared the relative expression of *RAD54L* in NDMM (N=14) with the relapsed MM (N=2), the RT-qPCR findings showed that *RAD54L* expression in relapsed MM was higher than NDMM, although the result was not significant (Fig. 1C).

The effects of *RAD54L* gene silencing on cell proliferation, apoptosis, cell cycle distribution and protein level in KMS-28BM MM cells

We have previously integrated the gene expression profiles with the miRNA expression profiles from the matched MM samples and revealed an inverse correlation between 5 putative target genes (*RAD54L*, *CCNA2*, *CYSLTR2*, *HKDC1* and *RASGRF2*) and 15 dysregulated miRNAs (Bong et al. 2017). Among the 5 genes listed, *RAD54L* is one of the new genes that has never been reported in association with MM. This prompted us to explore the in vitro function of *RAD54L* in MM cells. Since the MM clinical samples used in this study were derived from the Asian population, we would like to study the function of *RAD54L* in MM cell lines derived from the same origin. Thus, we have selected KMS-28BM as a model for functional analysis: a cell line which showed the highest *RAD54L* expression level among the 3 cell lines derived from Asian patients included for the gene expression profiling (Fig. 2A).

Silencing of *RAD54L* gene with siRNA duplexes successfully knockdown *RAD54L* expression in KMS-28BM by 71% at 24 h post-transfection as measured by RT-qPCR ($P < 0.05$) (Fig. 2B). The MTS assay revealed significant decreased in proliferation of MM cells treated with *RAD54L* siRNA compared to the control siRNA at 48 h ($P < 0.01$) and 72 h ($P < 0.05$) post-transfection (Fig. 2C). Flow cytometry results showed that silencing of *RAD54L* led to a small but significant increase in the numbers of early apoptotic cells in siRNA-treated cells compared to the control siRNA-treated cells ($P < 0.01$) (Fig. 2D). Additionally, cell cycle analysis showed that gene silencing of *RAD54L* significantly induced cell cycle arrest at G0/G1 phase ($P < 0.01$) while reduced S phase ($P < 0.05$) in KMS-28BM (Fig. 2E). ELISA results

showed that *RAD54L* protein expression diminished by approximately 19% with *RAD54L* knockdown at 48 h post-transfection ($P < 0.05$) (Fig. 2F).

Discussion

MM is a highly heterogeneous and complex disease which develops via a stepwise process involving multiple genetic aberrations. Numerous genetic aberrations have been identified in association with MM development and malignancy. However, to date MM is still an incurable disease mainly because most of the patients eventually relapse or are refractory to the available treatments (Davis and Sherbenou 2021). Thus, identification of new molecular targets is urgently needed to solve this problem.

Herein, we used mRNA expression profiling to identify potential genes involved in the molecular pathogenesis of MM. Unsupervised hierarchical clustering analysis of the up-regulated and down-regulated probes clearly clustered the samples into MM cell lines, MM clinical samples (except MM9 for the up-regulated probes and MM5 & MM9 for the down-regulated probes) and control groups (Online Resources 3 & 4). This scenario depicts that gene expression changes occur during the transition from normal to malignant plasma cells (Szalat et al. 2016). This study identified a total of 5124 DEGs in the MM vs. control group. Our findings revealed up-regulation of recurrent genes involved in primary oncogenic events: *CCND1* and *FGFR3* (Kuehl and Bergsagel 2012). Prominent and potential genes involved in the secondary oncogenic event such as *NRAS*, *IRF4*, *IDH2*, *PSMB5* and *APOBEC2* were found to be up-regulated whereas *SP140*, *LTB* and *ATM* were down-regulated in MM (Kuehl and Bergsagel 2012; Bolli et al. 2014; Walker et al. 2018; Allmeroth et al. 2021). Apart from that, differential expression of genes involved in NF- κ B pathway were identified (*NFKB1B*, *IKBKB*, *CARD11*, *TNFRSF1A*, *MAP3K1*, *MAP3K14* and *TLR4*) suggesting the important role of NF- κ B pathway in myelomagenesis (Chapman et al. 2011). Aberrant expression of apoptosis-related genes such as *BCL2*, *BIK* and *BAX* were also detected in the current study (Gupta et al. 2021). Additionally, the most established growth factors and cytokines involved in bone marrow microenvironment, namely *IL6* and *IGF1*, were found to be over-expressed in the MM vs. control group in this study (Birmann et al. 2009). Other DEGs, namely *BIRC5*, *CENPA*, *CCNB1*, *CHEK1*, *AURKB*, *BUB1*, *BUB1B*, *NEK2*, *ASPM*, *TOP2A* and *EZH2* have been described elsewhere and they play a role, at least in part, in the molecular pathogenesis of MM (Chng and Fonseca 2009; Broyl et al. 2010; Chung et al. 2013). Our findings revealed that most of the DEGs are involved in DNA repair, cell proliferation, cell cycle and mitotic/spindle checkpoints, mismatch repair pathway,

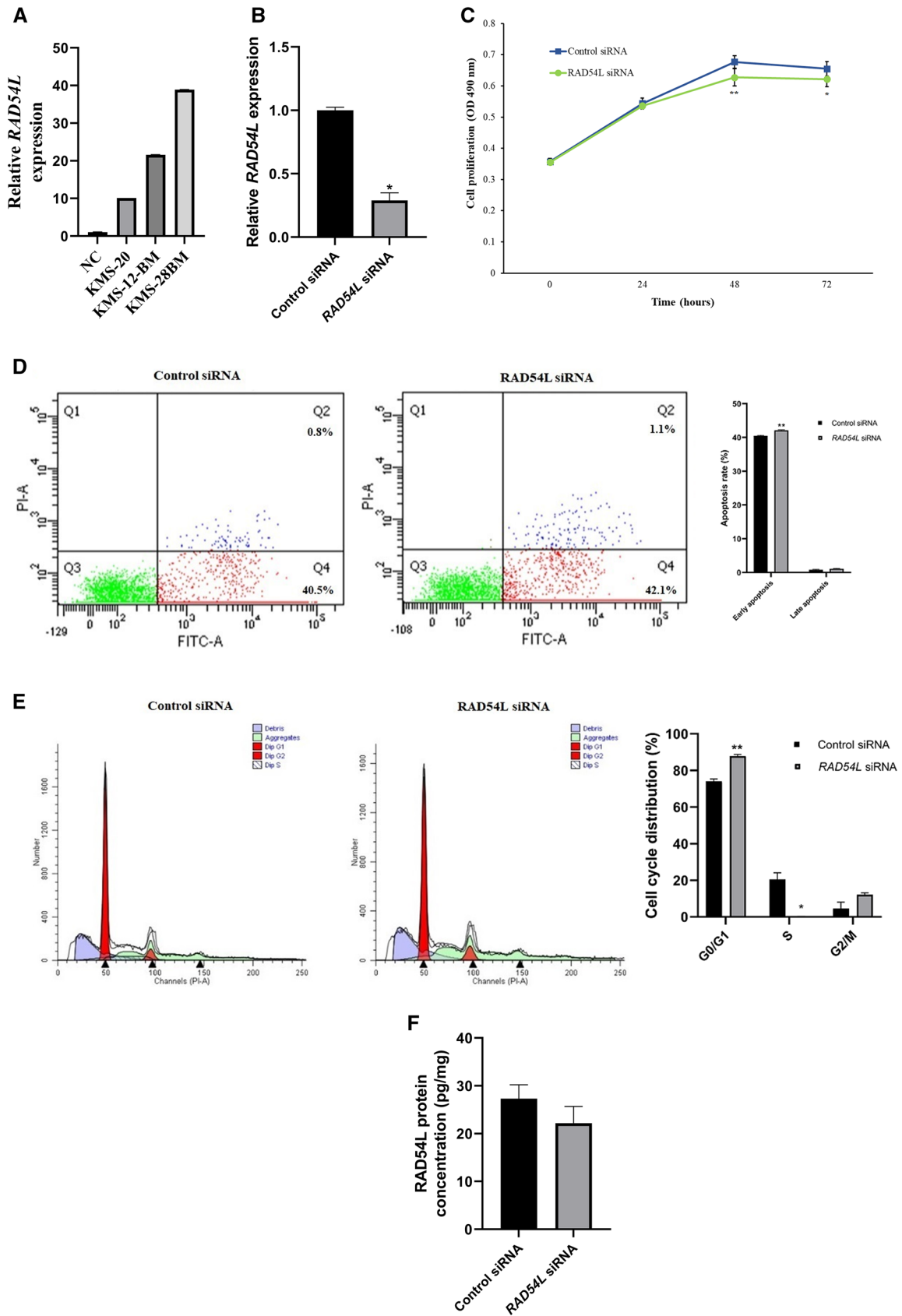


Fig. 2 **A** Graph showing relative *RAD54L* expression in KMS-20, KMS-12BM and KMS-28BM MM cell lines as measured by RT-qPCR. **B** Relative *RAD54L* expression was reduced by 71% in *RAD54L* siRNA-treated vs. control siRNA-treated KMS-28BM cells at 24 h post-transfection as measured by RT-qPCR. **C** Cell proliferation was decreased in KMS-28BM cells transfected with *RAD54L* siRNA compared to control siRNA at 48 h and 72 h post-transfection as analysed by MTS assay. **D** Number of early apoptotic cells showing small but significant increase in KMS-28BM cells transfected with *RAD54L* siRNA compared to control siRNA at 48 h post-transfection as analysed by flow cytometry. **E** *RAD54L* gene silencing significantly induced cell cycle arrest at G0/G1 phase while reduced S phase in *RAD54L* siRNA-treated cells compared to control at 48 h post-transfection as determined by flow cytometry. **F** *RAD54L* protein expression level was decreased by approximately 19% in KMS-28BM cells transfected with *RAD54L* siRNA compared to control siRNA at 48 h post-transfection as measured by ELISA assay. * $P < 0.05$; ** $P < 0.01$

kinetochore and microtubule attachment and NF- κ B pathway (Chng et al. 2006; Ueki et al. 2008; Chng and Fonseca 2009; Ruiz et al. 2009; Broyl et al. 2010; Agarwal et al. 2011; Chapman et al. 2011; Asano et al. 2013; Bengtsson et al. 2013; Chung et al. 2013; Jiao et al. 2013; Li and Huang 2013; Chuang and Ou 2014; Morley et al. 2015; Perez-Peña et al. 2017; Contreras et al. 2019; Ji et al. 2019; Xia et al. 2020; Borah and Reddy 2021; Li et al. 2021). DEGs and their functions are shown in Table 2.

Interestingly, our study reveals significant DEGs, which have never been reported in association with myelomagenesis. They are *RAD54L*, *DIAPH3*, *SHCBP1*, *SKA3*, *ANLN*, *HKDC1*, *RASGRF2* and *CYSLTR2*. The *RAD54L*, *DIAPH3*, *SHCBP1*, *SKA3* and *ANLN* were up-regulated while *HKDC1*, *RASGRF2* and *CYSLTR2* were down-regulated in MM vs. controls. Over-expression of *RAD54L* was detected in the MM vs. control group in this study by 18.3-folds. We then verified the expression of *RAD54L* in 23 samples by using RT-qPCR and the results are consistent with microarray analysis. *RAD54L* is involved in homologous recombination repairing of DNA double-strand breaks to facilitate human genomic integrity and genetic diversity (Andriuskevicius et al. 2018). Defects in homologous recombination pathway-related genes *RAD54*, *RAD51* and *RAD52* could lead to tumour development (Mun et al. 2020). *RAD54* interacts with *RAD51* nucleoprotein filament to form *RAD54*-*RAD51*-ssDNA nucleoprotein complex to stimulate homology search and DNA strand exchange (Zohud et al. 2020). *RAD54* also removes *RAD51* from heterodimeric DNA in an ATP-dependent manner after DNA strand exchange (Andriuskevicius et al. 2018; Rosenbaum et al. 2019). In G2 phase of the cell cycle, *RAD54* is phosphorylated to remove *RAD51* to facilitate homologous recombination while it is not phosphorylated in S phase to allow *RAD51* stabilizing and protecting the stalled replication forks from nucleolytic degradation (Spies et al. 2016). Thus, *RAD54* deficiency reduces homologous recombination efficiency. In addition

to *RAD54L*, our results revealed up-regulation of *RAD51* (13.8-folds), implicating that the deficiency in the homologous recombination pathway plays a critical role, at least in part, in the pathogenesis of MM.

Elevated expression of *RAD54L* is detected in carcinomas of the breast, colon, lymphoma and meningioma; however, its role in MM pathogenesis is unknown (Leone et al. 2003). In colorectal carcinoma, *RAD54L* taking part in maintaining chromosomal stability via DNA homologous recombination and p53 signalling pathway by interacting with *POLE* (Zohud et al. 2020). Apart from p53 pathway, *RAD54L* also interacting with other genes such as *E2F1* and *NEK2* in tumorigenesis (Mun et al. 2020; Pavan et al. 2021). Interestingly, *E2F1* and *NEK2* were found to be up-regulated in the MM vs. control group in this study by 14.2 and 21.8-folds, respectively. *E2F1* is a well-recognized transcription factor that regulates cell cycle progression in the suppression of tumorigenesis, whereas *NEK2* is involved in maintaining the stability of replication forks (Karras et al. 2016; Pavan et al. 2021).

The p53-DREAM pathway is a newly described p53-mediated cell cycle arrest pathway. The p53-DREAM pathway regulates not only cell cycle associated genes essential for cell cycle progression from G1 phase to the end of mitosis, but also DNA repair and telomere maintenance genes (Fischer et al. 2014; Engeland 2018). Thus, defects in this pathway lead to the loss of checkpoint control and uncontrolled cell division (Engeland 2018). Apart from that, aberrant expression of genes in this pathway induces chromosomal instability and aneuploidy in cancer cells (Thompson and Compton 2010). To date, almost 250 target genes regulated by the p53-DREAM pathway have been identified (Fischer et al. 2014; Engeland 2018). Interestingly, *RAD54L* and many other DEGs that function in cell cycle or checkpoint control identified in the current study are components of the p53-DREAM pathway (*CCNA2*, *BIRC5*, *CENPA*, *CENPF*, *CCNB1*, *CCNB2*, *CDC25C*, *KIF14*, *DEPDC1* and *CDK1*) (Table 2) (Fischer et al. 2014; Engeland 2018). *CCNA2*, *BIRC5*, *CCNB1*, *CCNB2*, *CDC25C* and *CDK1* are key regulators in the p53-DREAM pathway (Fischer et al. 2015, 2016). It was postulated that *RAD54L*, *CCNA2* and *CCNB1* are p53-dependent repression of the cell cycle genes, in which they contain cell cycle genes homology region (CHR) elements that allow them to bind with DREAM transcriptional repressor (Fischer et al. 2014, 2016). Most of these target genes are involved in G2/M checkpoint control and progression through mitosis (Fischer et al. 2016). Our results indicate that disruption of the p53-DREAM pathway plays a critical role in MM pathogenesis as many genes involved in this pathway were differentially expressed in MM.

In terms of epigenetic aspect, our previous findings on the integrative analysis of the mRNA and miRNA expression

Table 2 Functions and fold changes of differentially expressed genes (DEGs)

Function	Gene symbol (fold change)
Cell cycle and cell cycle checkpoint	<i>CCNA2</i> (20.6), <i>BIRC5</i> (32.0), <i>CENPA</i> (39.0), <i>CENPF</i> (18.4), <i>CCNB1</i> (10.5), <i>CCNB2</i> (33.0), <i>CDC25C</i> (19.0), <i>KIF14</i> (29.1), <i>DEPDC1</i> (13.3), <i>CDK1</i> (18.7), <i>CCND1</i> (7.8)
DNA repair	<i>RAD54L</i> (18.3), <i>RAD51AP1</i> (26.0), <i>RAD51</i> (13.8), <i>CHEK1</i> (11.2), <i>ATM</i> (-3.5)
Mitotic/spindle checkpoints	<i>PLK1</i> (17.1), <i>NUF2</i> (17.7), <i>AURKB</i> (20.9), <i>CDC20</i> (11.8), <i>BUB1</i> (18.7), <i>BUB1B</i> (24.0), <i>CENPA</i> (39.0), <i>NEK2</i> (21.8), <i>TTK</i> (41.1), <i>TK1</i> (23.2), <i>CKAP2L</i> (43.0), <i>KIF11</i> (14.7), <i>KIF20A</i> (35.0), <i>SKA1</i> (40.8), <i>TPX2</i> (22.3), <i>DTL</i> (33.1)
Cell proliferation	<i>ASPM</i> (27.2), <i>TOP2A</i> (23.8), <i>TTK</i> (41.1), <i>E2F1</i> (14.2), <i>E2F7</i> (18.5), <i>E2F8</i> (33.4), <i>CDCA8</i> (13.4), <i>SHCBP1</i> (19.6), <i>FGFR3</i> (20.2), <i>PSMB5</i> (2.2), <i>ATM</i> (-3.6)
Kinetochores and microtubule attachment	<i>ZWINT</i> (13.6), <i>AURKB</i> (20.9), <i>BIRC5</i> (32.0), <i>CENPA</i> (39.0), <i>TTK</i> (41.1), <i>KIF2C</i> (27.0), <i>SKA3</i> (20.2)
Apoptosis	<i>BCL2</i> (-2.9), <i>BIK</i> (3.6), <i>BAX</i> (2.2)
Growth factor	<i>IL6</i> (15.6), <i>IGF1</i> (9.2), <i>IGF2</i> (18.6)
Mismatch repair pathway	<i>PCNA</i> (5.9)
Centrosome	<i>KIF11</i> (14.7), <i>KIF15</i> (20.2), <i>AURKB</i> (20.9)
Chromatin regulator	<i>SPI40</i> (-3.1)
Ubiquitin proteasome	<i>UBE2S</i> (6.1), <i>UBE2T</i> (11.5)
Cytokine	<i>IRF4</i> (3.3)
Metabolism	<i>HKDC1</i> (-9.3), <i>IDH2</i> (2.2)
Cytoskeleton	<i>DIAPH3</i> (19.6), <i>ANLN</i> (44.1)
TNF-associated gene	<i>LTB</i> (-9.6)
Polycomb	<i>EZH2</i> (5.6)
NFκB pathway	<i>IKBKB</i> (-3.1), <i>NFKBIB</i> (2.0), <i>CARD11</i> (-2.9), <i>TNFRSF1A</i> (-4.5), <i>MAP3K1</i> (-2.0), <i>MAP3K14</i> (-2.3), <i>TLR4</i> (-6.8)
RAS related pathway	<i>NRAS</i> (2.3), <i>RASGRF2</i> (-5.5)
CysLT signaling	<i>CYSLTR2</i> (-7.3)
APOBEC-associated genes	<i>APOBEC2</i> (2.6), <i>APOBEC3G</i> (-2.1)
Histone	<i>HIST1H2BI</i> (2.3), <i>HIST1H2BK</i> (2.1), <i>HIST1H2BL</i> (2.1), <i>HIST1H2BM</i> (2.1), <i>HIST1H2BB</i> (2.8), <i>HIST1H2BD</i> (2.1), <i>HIST1H2BE</i> (3.1), <i>HIST1H2BF</i> (5.4), <i>HIST1H2BG</i> (2.5), <i>HIST1H2BH</i> (2.1), <i>HIST3H2BB</i> (2.8), <i>HIST1H3H</i> (3.5), <i>HIST2H3A</i> (42.6), <i>HIST1H3B</i> (9.6), <i>HIST1H3D</i> (4.0), <i>HIST1H3F</i> (4.3), <i>HIST1H3G</i> (2.4), <i>HIST1H4A</i> (3.6), <i>HIST1H4K</i> (2.3), <i>HIST1H4L</i> (3.7), <i>HIST1H4B</i> (3.5), <i>HIST1H4C</i> (3.1), <i>HIST1H4D</i> (3.9)

profiling for matched samples revealed an inverse correlation between *RAD54L* and cancer-associated miR-150 (Bong et al. 2017). Based on computational predictions, our previous findings revealed that differential expression of *RAD54L* might be correlated with aberrant expression of miR-150-5p, which regulates the gene. Thus, according to our observation, we suggest that *RAD54L* possibly triggers MM either independently or by interacting with other genes/miRNA via impairing DNA repair mechanism and cell cycle progression.

To validate the function of *RAD54L* in MM, we transiently knockdown *RAD54L* in KMS-28BM human MM cell line using siRNA method. The effects of *RAD54L*-mediated gene silencing on cell proliferation, apoptosis and cell cycle distribution in KMS-28BM were determined. Our results reveal that gene silencing of *RAD54L* inhibits cell proliferation in KMS-28BM (Fig. 2C). In addition, *RAD54L* knockdown induces small but significant changes in early apoptotic cells (Fig. 2D). Moreover, cell cycle analysis demonstrates that depletion of *RAD54L* induces cell cycle arrest at G0/G1 phase and inhibits cells at S phase suggesting that *RAD54L* is involved in cell

cycle progression (Fig. 2E). The ELISA assay shows that silencing of *RAD54L* not only knockdown the gene expression at the mRNA level but also decreases its protein expression level (Fig. 2F). For the first time, our results demonstrate that up-regulation of *RAD54L* might play a key role, at least in part, in MM pathogenesis by activating myeloma cell growth, inhibiting apoptosis and impairing cell cycle progression.

The limitation of the present study is the small number of samples used for gene expression profiling, which may reduce the statistical power of the study. Our future direction is to validate the results with larger sample sizes by using a more advanced technology such as RNA-sequencing (RNA-seq).

Conclusions

This study has identified possible molecular targets underlying MM pathogenesis. *RAD54L* might be a potential therapeutic target in MM, possibly functioning in the cell cycle and checkpoint control.

Supplementary Information The online version contains supplementary material available at <https://doi.org/10.1007/s13258-022-01272-7>.

Acknowledgements The authors would like to thank the Director General of Health, Ministry of Health Malaysia for approval to publish this research paper. We would also like to thank the Deputy Director General of Health (Research and Technical Support) and the Director of the Institute for Medical Research (IMR) for their support in the publication of this paper.

Author contributions Conceptualisation: IPNB; formal analysis: IPNB; methodology: IPNB, NO; funding acquisition: IPNB; writing—original draft: IPNB; writing—review and editing: IPNB, CCN; final approval of the version to be published: EE.

Funding This study was funded by a research grant from the Ministry of Health Malaysia (NMRR-18-729-41414), awarded to Bong IPN.

Data availability The microarray-generated gene expression data can be retrieved from NCBI Gene Expression Omnibus (GEO) repository as series accession identifier GSE72213.

Declarations

Conflict of interest Bong IPN, Ng CC, Othman N and Esa E declare that they have no conflict of interest.

Ethical approval This study was approved by the Medical Research & Ethics Committee (MREC), Ministry of Health, Malaysia. Informed consent was obtained from all subjects recruited in the study.

Open Access This article is licensed under a Creative Commons Attribution 4.0 International License, which permits use, sharing, adaptation, distribution and reproduction in any medium or format, as long as you give appropriate credit to the original author(s) and the source, provide a link to the Creative Commons licence, and indicate if changes were made. The images or other third party material in this article are included in the article's Creative Commons licence, unless indicated otherwise in a credit line to the material. If material is not included in the article's Creative Commons licence and your intended use is not permitted by statutory regulation or exceeds the permitted use, you will need to obtain permission directly from the copyright holder. To view a copy of this licence, visit <http://creativecommons.org/licenses/by/4.0/>.

References

- Agarwal S, van Cappellen WA, Guérolé A, Eppink B, Linsen SEV, Meijering E (2011) ATP-dependent and independent functions of Rad54 in genome maintenance. *J Cell Biol* 192(5):735–750. <https://doi.org/10.1083/jcb.201011025>
- Allmeroth K, Horn M, Kroef V, Mieth S, Müller RU, Denzel MS (2021) Bortezomib resistance mutations in PSMB5 determine response to second-generation proteasome inhibitors in multiple myeloma. *Leukemia* 35(3):887–892. <https://doi.org/10.1038/s41375-020-0989-4>
- Andriuskevicius T, Kotenko O, Makovets S (2018) Putting together and taking apart: assembly and disassembly of the Rad51 nucleoprotein filament in DNA repair and genome stability. *Cell Stress* 2(5):96–112. <https://doi.org/10.15698/cst2018.05.134>

- Asano E, Hasegawa H, Hyodo T, Ito S, Maeda M, Takahashi M, Hamauchi M, Senga T (2013) The Aurora B-mediated phosphorylation of SHCBP1 regulates cytokinetic furrow ingression. *J Cell Sci* 126(Pt 15):3263–3270. <https://doi.org/10.1242/jcs.124875>
- Bengtsson AM, Jönsson G, Magnusson C, Salim T, Axelsson C, Sjölander A (2013) The cysteinyl leukotriene 2 receptor contributes to all-trans retinoic acid-induced differentiation of colon cancer cells. *BMC Cancer* 13:336. <https://doi.org/10.1186/1471-2407-13-336>
- Birmann BM, Tamimi RM, Giovannucci E, Rosner B, Hunter DJ, Kraft P, Mitsiades C, Anderson KC, Colditz GA (2009) Insulin-like growth factor-1- and interleukin-6-related gene variation and risk of multiple myeloma. *Cancer Epidemiol Biomarkers Prev* 18(1):282–288. <https://doi.org/10.1158/1055-9965>
- Bolli N, Avet-Loiseau H, Wedge DC, Van Loo P, Alexandrov LB, Martincorena I, Dawson KJ, Iorio F, Nik-Zainal S, Bignell GR et al (2014) Heterogeneity of genomic evolution and mutational profiles in multiple myeloma. *Nat Commun* 5:2997. <https://doi.org/10.1038/ncomms3997>
- Bong IPN, Ng CC, Baharuddin P, Zakaria Z (2017) MicroRNA expression patterns and target prediction in multiple myeloma development and malignancy. *Genes Genomics* 39(5):533–540. <https://doi.org/10.1007/s13258-017-0518-7>
- Borah NA, Reddy MM (2021) Aurora kinase B inhibition: a potential therapeutic strategy for cancer. *Molecules* 26(7):1981. <https://doi.org/10.3390/molecules26071981>
- Broyl A, Hose D, Lokhorst H, Peeters J, Jauch A, Bertsch U, Buijs A, Stevens-Kroef M, Beverloo HB, Vellenga E et al (2010) Gene expression profiling for molecular classification of multiple myeloma in newly diagnosed patients. *Blood* 116(14):2543–2553. <https://doi.org/10.1182/blood-2009-12-261032>
- Chapman MA, Lawrence MS, Keats JJ, Cibulskis K, Sougnez C, Schinzel AC, Harview CL, Brunet JP, Ahmann GJ, Adli M et al (2011) Initial genome sequencing and analysis of multiple myeloma. *Nature* 471(7339):467–472. <https://doi.org/10.1038/nature09837>
- Chng WJ, Fonseca R (2009) Centrosomes and myeloma; aneuploidy and proliferation. *Environ Mol Mutagen* 50(8):697–707. <https://doi.org/10.1002/em.20528>
- Chng W-J, Baker A, Henry T, Price-Troska T, van Wier S, Chung T-H (2006) Combined high resolution array comparative genomic hybridization and gene expression profiling reveal *rb1* haploinsufficiency as a possible tumorigenic mechanism in myeloma. *Blood* 108(11):113. <https://doi.org/10.1182/blood.V108.11.113.113>
- Chuang HY, Ou YH (2014) Overexpression of anillin in colorectal cancer promotes the cell proliferation, cell mobility and cell invasion. *Cancer Res* 74(19):4068. <https://doi.org/10.1158/1538-7445.AM2014-4068>
- Chung T-H, Mulligan G, Fonseca R, Chng WJ (2013) A novel measure of chromosome instability can account for prognostic difference in multiple myeloma. *PLoS ONE* 8(6):e66361. <https://doi.org/10.1371/journal.pone.0066361>
- Colombo M, Galletti S, Garavelli S, Platonova N, Paoli A, Basile A, Taiana E, Neri A, Chiaramonte R (2015) Notch signaling deregulation in multiple myeloma: a rational molecular target. *Oncotarget* 6(29):26826–26840. <https://doi.org/10.18632/oncotarget.5025>
- Contreras J, Caldas-Lopes E, Jayabalan D, Monge J, Lombardi N, Li H-y, Gunaganti N, Niesvizky R, Guzman N (2019) Targeting Aurora-kinase B with the novel Aurora Kinase B inhibitor MK7 in multiple myeloma. *Clin Lymphoma Myeloma Leuk* 19(10):e128. <https://doi.org/10.1016/j.clml.2019.09.212>
- Corre J, Munshi N, Avet-Loiseau H (2015) Genetics of multiple myeloma: another heterogeneity level? *Blood* 125(12):1870–1876. <https://doi.org/10.1038/sj.leu.2404621>

- Davis LN, Sherbenou DW (2021) Emerging therapeutic strategies to overcome drug resistance in multiple myeloma. *Cancers (basel)* 13(7):1686. <https://doi.org/10.3390/cancers13071686>
- de Mel S, Lim SH, Tung ML, Chng W-J (2014) Implications of heterogeneity in multiple myeloma. *Biomed Res Int* 2014:232546. <https://doi.org/10.3390/ijms20051248>
- Engeland K (2018) Cell cycle arrest through indirect transcriptional repression by p53: I have a DREAM. *Cell Death Differ* 25(1):114–132. <https://doi.org/10.1038/cdd.2017.172>
- Fischer M, Steiner L, Engeland K (2014) The transcription factor p53: not a repressor, solely an activator. *Cell Cycle* 13(19):3037–3058. <https://doi.org/10.4161/15384101.2014.949083>
- Fischer M, Quaas M, Nickel A, Engeland K (2015) Indirect p53-dependent transcriptional repression of Survivin, CDC25C, and PLK1 genes requires the cyclin-dependent kinase inhibitor p21/CDKN1A and CDE/CHR promoter sites binding the DREAM complex. *Oncotarget* 6(39):41402–41417. <https://doi.org/10.18632/oncotarget.6356>
- Fischer M, Quaas M, Steiner L, Engeland K (2016) The p53–p21–DREAM–CDE/CHR pathway regulates G2/M cell cycle genes. *Nucleic Acids Res* 44(1):164–174. <https://doi.org/10.1093/nar/gkv927>
- Furukawa Y, Kikuchi J (2020) Molecular basis of clonal evolution in multiple myeloma. *Int J Hematol* 111(4):496–511. <https://doi.org/10.1007/s12185-020-02829-6>
- Gupta VA, Ackley J, Kaufman JL, Boise LH (2021) BCL2 family inhibitors in the biology and treatment of multiple myeloma. *Blood Lymphat Cancer* 11:11–24. <https://doi.org/10.2147/BLCTT.S245191>
- Ji C, Ma J, Shu P (2019) Effect of denticleless e3 ubiquitin protein ligase on proliferation and clone formation of multiple myeloma cells. *Zhongguo Yi Xue Ke Xue Yuan Xue Bao* 41(2):194–202. <https://doi.org/10.3881/j.issn.1000-503X.10674>
- Jiao X, Hooper SD, Djureinovic T, Larsson C, Wärnberg F, Tellgren-Roth C, Botling J, Sjöblom T (2013) Gene rearrangements in hormone receptor negative breast cancers revealed by mate pair sequencing. *BMC Genomics* 14:165. <https://doi.org/10.1186/1471-2164-14-165>
- Karras JR, Schrock MS, Batar B, Huebner K (2016) Fragile genes that are frequently altered in cancer: players not passengers. *Cytogenet Genome Res* 150(3–4):208–216. <https://doi.org/10.1159/000455753>
- Kuehl WM, Bergsagel PL (2012) Molecular pathogenesis of multiple myeloma and its premalignant precursor. *J Clin Invest* 122(10):3456–3463. <https://doi.org/10.1172/JCI61188>
- Leone PE, Mendiola M, Alonso J, Paz-y-Miño C, Pestaña A (2003) Implications of a RAD54L polymorphism (2290C/T) in human meningiomas as a risk factor and/or a genetic marker. *BMC Cancer* 3:6. <https://doi.org/10.1186/1471-2407-3-6>
- Li G-H, Huang J-F (2013) Inferring therapeutic targets from heterogeneous data: HKDC1 is a novel potential therapeutic target for cancer. *Bioinformatics* 30(6):748–752. <https://doi.org/10.1093/bioinformatics/btt606>
- Li C, Wendlandt EB, Darbro B, Xu H, Thomas GS, Tricot G, Chen F, Shaughnessy JD Jr, Zhan F (2021) Genetic analysis of multiple myeloma identifies cytogenetic alterations implicated in disease complexity and progression. *Cancers (basel)* 13(3):517. <https://doi.org/10.3390/cancers13030517>
- Morley S, You S, Pollan S, Choi J, Zhou B, Hager MH, Steadman K, Spinelli C, Rajendran K, Gertych A et al (2015) Regulation of microtubule dynamics by DIAPH3 influences amoeboid tumor cell mechanics and sensitivity to taxanes. *Sci Rep* 5:12136. <https://doi.org/10.1038/srep12136>
- Mun J-Y, Baek S-W, Park WY, Kim W-T, Kim S-K, Roh Y-G, Jeong M-S, Yang G-E, Lee J-H, Chung JW et al (2020) E2F1 promotes progression of bladder cancer by modulating RAD54L involved in homologous recombination repair. *Int J Mol Sci* 21(23):9025. <https://doi.org/10.3390/ijms21239025>
- Pavan ICB, Peres de Oliveira A, Dias PRF, Basei FL, Issayama LK, Ferezin C, Silva FR, Rodrigues de Oliveira AL, Dos Reis A, Moura L, Martins MB et al (2021) On broken ne(c)ks and broken DNA: the role of human NEKs in the DNA damage response. *Cells* 10(3):507. <https://doi.org/10.3390/cells10030507>
- Perez-Peña J, Corrales-Sánchez V, Amir E, Pandiella A, Ocana A (2017) Ubiquitin-conjugating enzyme E2T (UBE2T) and denticleless protein homolog (DTL) are linked to poor outcome in breast and lung cancers. *Sci Rep* 7:17530. <https://doi.org/10.1038/s41598-017-17836-7>
- Pinto V, Bergantim R, Caires HR, Seca H, Guimarães JE, Vasconcelos MH (2020) Multiple myeloma: available therapies and causes of drug resistance. *Cancers (basel)* 12(2):407. <https://doi.org/10.3390/cancers12020407>
- Rosenbaum JC, Bonilla B, Hengel SR, Mertz TM, Herken BW, Kazemier HG, Pressimone CA, Ratterman TC, MacNary E, De Magis A et al (2019) The Rad51 paralogs facilitate a novel DNA strand specific damage tolerance pathway. *Nat Commun* 10:3515. <https://doi.org/10.1038/s41467-019-11374-8>
- Roy P, Sarkar UA, Basak S (2018) The NF- κ B activating pathways in multiple myeloma. *Biomedicines* 6(2):59. <https://doi.org/10.3390/biomedicines6020059>
- Ruiz S, Santos E, Bustelo XR (2009) The use of knockout mice reveals a synergistic role of the Vav1 and Rasgrf2 gene deficiencies in lymphomagenesis and metastasis. *PLoS ONE* 4(12):e8229. <https://doi.org/10.1371/journal.pone.0008229>
- Spies J, Waizenegger A, Barton O, Sürder M, Wright WD, Heyer W-D, Löbrich M (2016) Nek1 regulates Rad54 to orchestrate homologous recombination and replication fork stability. *Mol Cell* 62(6):903–917. <https://doi.org/10.1016/j.molcel.2016.04.032>
- Szalat R, Avet-Loiseau H, Munshi NC (2016) Gene expression profiles in myeloma: ready for the real world? *Clin Cancer Res* 22(22):5434–5442. <https://doi.org/10.1158/1078-0432.CCR-16-0867>
- Thompson SL, Compton DA (2010) Proliferation of aneuploid human cells is limited by a p53-dependent mechanism. *J Cell Biol* 188(3):369–381. <https://doi.org/10.1083/jcb.200905057>
- Ueki T, Nishidate T, Park JH, Lin ML, Shimo A, Hirata K, Nakamura Y, Katagiri T (2008) Involvement of elevated expression of multiple cell-cycle regulator, DTL/RAMP (denticleless/RA-regulated nuclear matrix associated protein), in the growth of breast cancer cells. *Oncogene* 27(43):5672–5683. <https://doi.org/10.1038/nc.2008.186>
- Walker BA, Mavrommatis K, Wardell CP, Ashby TC, Bauer M, Davies FE, Rosenthal A, Wang H, Qu P, Hoering A et al (2018) Identification of novel mutational drivers reveals oncogene dependencies in multiple myeloma. *Blood* 132(6):587–597. <https://doi.org/10.1182/blood-2018-03-840132>
- Xia J, He Y, Meng B, Chen S, Zhang J, Wu X, Zhu Y, Shen Y, Feng X, Guan Y et al (2020) NEK2 induces autophagy-mediated bortezomib resistance by stabilizing Beclin-1 in multiple myeloma. *Mol Oncol* 14(4):763–778. <https://doi.org/10.1002/1878-0261>
- Zohud BA, Wang M, Cai X (2020) Germline RAD54L with somatic POLE defect implicated in Hypermutation phenotype: case report. *BMC Gastroenterol* 20:255. <https://doi.org/10.1186/s12876-020-01403-y>

Publisher's Note Springer Nature remains neutral with regard to jurisdictional claims in published maps and institutional affiliations.